Virtual edge illumination and one dimensional beam tracking for absorption, refraction, and scattering retrieval

Fabio A. Vittoria,[1,2,a)] Marco Endrizzi,[1] Paul C. Diemoz,[1,2] Ulrich H. Wagner,[3] Christoph Rau,[3] Ian K. Robinson,[2,4] and Alessandro Olivo[1]

[1]*Department of Medical Physics and Bioengineering, University College London, Malet Place, Gower Street, London WC1E 6BT, United Kingdom*
[2]*Research Complex at Harwell, Harwell Oxford Campus, OX11 0FA Didcot, United Kingdom*
[3]*Diamond Light Source, Harwell Oxford Campus, OX11 0DE Didcot, United Kingdom*
[4]*London Centre for Nanotechnology, WC1H 0AH London, United Kingdom*

We propose two different approaches to retrieve x-ray absorption, refraction, and scattering signals using a one dimensional scan and a high resolution detector. The first method can be easily implemented in existing procedures developed for edge illumination to retrieve absorption and refraction signals, giving comparable image quality while reducing exposure time and delivered dose. The second method tracks the variations of the beam intensity profile on the detector through a multi-Gaussian interpolation, allowing the additional retrieval of the scattering signal. © 2014 Author(s). All article content, except where otherwise noted, is licensed under a Creative Commons Attribution 3.0 Unported License. [http://dx.doi.org/10.1063/1.4870528]

X-ray phase contrast imaging (XPCi) has been the subject of intense studies over the last decades.[1–6] Through XPCi, it is possible to obtain images of a sample in which the contrast is generated not only by x-ray attenuation, like in conventional radiography, but also by the phase shift which originates when radiation propagates inside a sample. Unfortunately, while absorption effects directly translate into a variation of the detected intensity, phase effects are usually more difficult to exploit. The phase contrast signal, in fact, can be strongly reduced by spatial[1,2,5,6] and temporal[1,3,5,6] incoherence of the source and by finite detector resolution.[2]

In an attempt to overcome these limitations, the Edge Illumination (EI) technique has been first developed at Elettra synchrotron[4] and then implemented with standard laboratory source[7] in the so called Coded Aperture (CA) configuration. In EI, the sample is scanned through a narrow laminar beam (Fig. 1). An absorbing edge, intercepting part of the beam, is placed in front of the detector, and the recorded intensity is integrated along the x direction. In the CA configuration, the pre-sample aperture and the detector edge are replaced by two masks, both with projected period equal to the detector pixel size. With both configurations, refraction induced shifts of the beam smaller than the pixel size cause a variation in the recorded intensities and can, thus, be detected. The interaction of the narrow beam with the sample can be seen, in a simple but effective description, as the result of three physical processes (Fig. 1): a decrease in the total intensity of the beam caused by absorption, a lateral shift (refraction) of the beam profile, proportional to the gradient of the phase shift induced by the sample, and a broadening of the beam (scattering) linked to inhomogeneities of the sample transmission function on a scale smaller than the beam width on the sample.[8] Absorption, refraction, and scattering thus contribute simultaneously to the contrast

of an EI image with relative weights that depend on the relative displacement between the edge and the beam. By acquiring a minimum of three images with different displacements and combining them together, it is possible to separate the absorption, refraction, and scattering signals.[9] In this letter, we will introduce two alternative approaches to the EI method, which can be implemented when a high resolution detector is available.

The first approach consists in removing the edge and recording the entire beam intensity with a high resolution detector. The edge is then simulated through a multiplication by a Heaviside function, and the resulting profile is integrated. This allows to simulate all the possible relative positions between this "virtual" edge and the beam from a single acquisition by shifting and/or inverting the Heaviside function. Figs. 2(a) and 2(b) show a comparison between the refraction signals of a polyetheretherketone (PEEK) monofilament of 160 μm diameter immersed in water, retrieved from data acquired in the "classical" (i.e., with an absorbing edge physically present) and virtual EI configurations. Experimental data were acquired at the beam line I13 (Coherence branch) of the Diamond Synchrotron Radiation (SR) facility (Didcot, UK). An x-ray energy of 9.7 keV was selected through a Si(111) crystal monochromator, and a 10 μm slit was used as presample aperture. The detector, placed at 58 cm from the
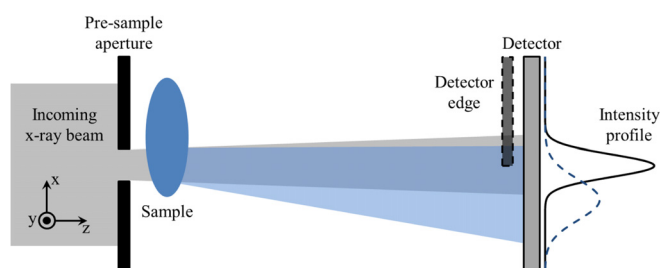

FIG. 1. Schematic diagram of an EI system.

a)Author to whom correspondence should be addressed. Electronic mail: fabio.vittoria.12@ucl.ac.uk
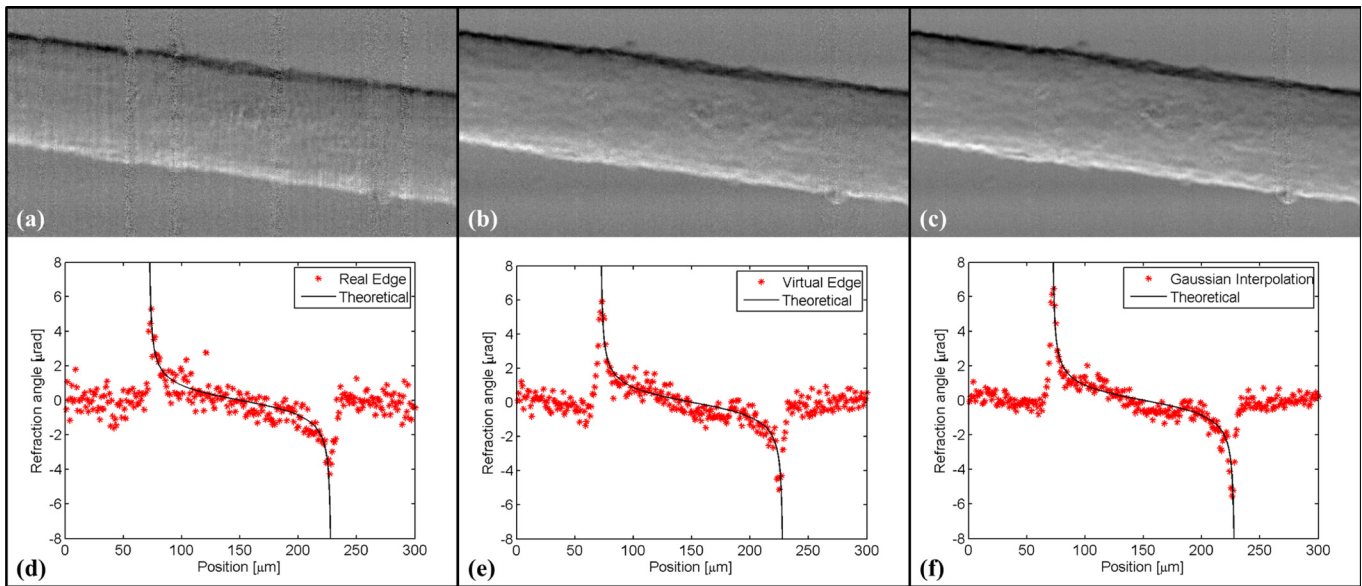
FIG. 2. Refraction signals of a PEEK monofilament immersed in water using the real (a) and virtual (b) edge configurations, and the beam tracking (c) method. In (d), (e), and (f), a vertical profile extracted from each image is compared to the theoretical refraction angle.

sample, consisted of a scintillator, a magnifying visible light optics and a CCD sensor, with effective pixel size of 0.8 μm. The difference in the absorption of PEEK and water at 9.7 keV is only 0.02%, and, for the sample in Fig. 2, the absorption signal is below the noise level in our acquisitions. Scattering is assumed to be negligible, and the procedure described in Ref. 10 was used for the retrieval. It should be noted that, in order to retrieve absorption and refraction, at least two images are required, with different positions of the absorbing edge.[10] Two separate scans of the sample are, therefore, needed with the classical EI, while with the virtual edge approach, two different Heaviside functions are applied to the same experimental dataset. This results in a similar image quality, but with a reduction of exposure time and delivered dose by a factor of 2 in the latter case. Most importantly, a single scan of the sample is performed, which minimizes the effects of possible sample movements (e.g., for *in vivo* or dynamic applications). Figs. 2(d) and 2(e) show the comparison between a vertical profile of the images (a) and (b), respectively, and the theoretical refraction angle: in both cases, a good agreement is found. The described approach has the advantage of being easily implementable in previously developed techniques for absorption and refraction retrieval.[10,11]

Originally, the EI technique was designed to detect beam variations on the detector by using an edge as analyser,[4] and the virtual edge approach implements the same concept via software. However, the beam intensity profile, and the changes it suffers when a sample is introduced, can be detected directly by the high resolution detector. The second approach we propose exploits this concept. It consists in tracking the beam variations in the x direction through interpolation techniques in order to reconstruct absorption, refraction, and scattering maps of the sample. A similar concept was presented in a 1995 patent by Wilkins,[12] where he proposed an adaptation of the Shack-Hartmann wavefront sensor for x-ray radiation. To the best of our knowledge, an implementation of this concept has never been realized in practice. However, recently other techniques have been

proposed to track the changes introduced by a sample to a known reference field by means of a high resolution detector.[13,14]

In our case, with reference to Fig. 1, the effects of absorption, refraction, and scattering on the recorded intensity profile can be mathematically formulated as[9]

$$I(x) = T I_0(x - \delta x) * s(x), \qquad (1)$$

where I and I_0 are the intensity patterns acquired with and without the sample, respectively, T is the fraction of the beam transmitted through the sample, δx is the lateral shift of the beam at the detector plane, and the effect of scattering is described by means of a convolution with the scattering function $s(x)$. When a CA configuration is used, as in Ref. 9, I and I_0 are not directly accessible, and only their convolution with the detector aperture, called illumination function L, can be measured. Nevertheless, the relation expressed in Eq. (1) still holds if I and I_0 are replaced by the illumination curves L and L_0 acquired with and without the sample, respectively. In Ref. 9, a normalized Gaussian distribution is assumed for $s(x)$, with standard deviation σ_S, and a Gaussian profile is also assumed for L_0; under these hypotheses, Eq. (1) can be solved analytically for T, δx, and σ_S by measuring L and L_0 for three different values of x, which in that case represents the relative displacement between the pre-sample and detector masks. If the same hypothesis is applied to the case in which I and I_0 are acquired with a high resolution detector, an over constrained problem is obtained that can be solved with a least square minimization approach, i.e., Gaussian interpolation of experimental data can be used to determine T, δx, and σ_S. In a more general case, I_0 can be assumed to be well approximated by a sum of Gaussian terms

$$I_0(x) = \sum_{n=1}^{N} A_n \exp\left[-\frac{(x - \mu_n)^2}{2\sigma_n^2}\right], \qquad (2)$$
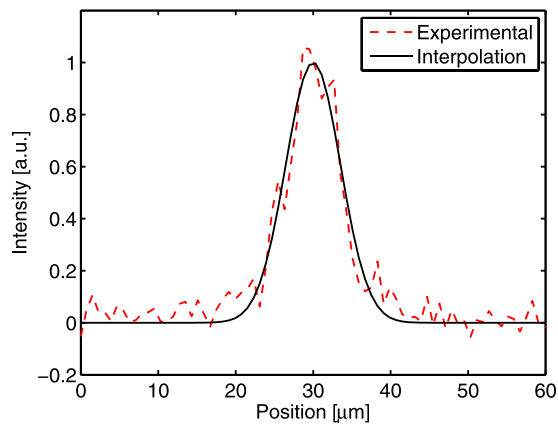
FIG. 3. Comparison between experimental and interpolated beam intensity profile.

FIG. 5. Colour rendering of the three signals in Fig. 4. Red represents absorption, blue the absolute value of refraction, and green scattering.

with the total number of terms N depending on the specific case. In the assumption of a normalized Gaussian distribution for $s(x)$, Eq. (1) becomes

$$I(x) = T \sum_{n=1}^{N} A_n \sqrt{\frac{\sigma_n^2}{\sigma_n^2 + \sigma_s^2}} \exp\left[-\frac{(x - \mu_n - \delta x)^2}{2(\sigma_n^2 + \sigma_S^2)}\right]. \quad (3)$$

T can be calculated from the ratio between the integrals of I and I_0 along x, while a N-Gaussian interpolation of I and I_0 allows retrieving δx and σ_S. Usually, the summations in Eqs. (2) and (3) present one dominant term which describes the general shape of the intensity profile, while the other terms provide a refinement of the interpolation. In principle, a better description of I and I_0 can be obtained by increasing the number of terms in Eqs. (2) and (3). However, in the practical cases we explored, one Gaussian term was enough to accurately interpolate the beam profile. An example of the adequacy of this approximation is shown in Fig. 3, where an experimental beam intensity profile is compared with the corresponding Gaussian fit.

We first applied the beam tracking method to the PEEK monofilament immersed in water. Figs. 2(c) and 2(f) show the retrieved refraction image and the comparison with the theoretical value, demonstrating a good agreement. We
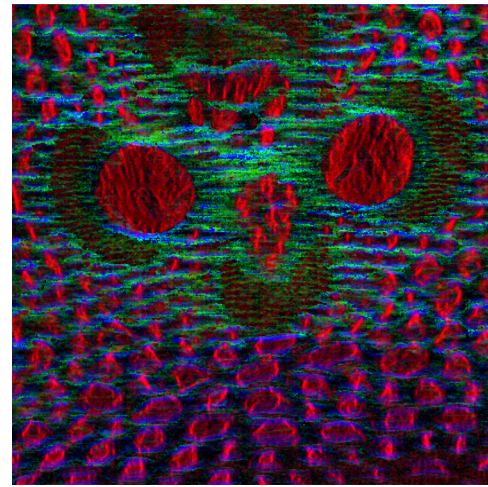
finally tested the method on a more complex sample, a bamboo wood slice of about $500\,\mu$m thickness from a "nature-inspired" engineering project currently ongoing at UCL. In this case, a $3\,\mu$m slit was used as pre-sample aperture, and the sample to detector distance was reduced to $30\,$cm. Fig. 4 shows the reconstructed absorption, refraction, and scattering signals. These images could also be fused together in, for example, a single RGB image (Fig. 5) to better appreciate the different contributions of the three signals. Each signal is in fact sensitive to different features of the object: usually absorption signal offers the best contrast for the low frequency part of the image, refraction is instead stronger at the edges of the sample structures, and scattering reveals the presence of strong variations in the sample transmission function not resolved in the absorption and refraction images.

In conclusion, we presented two new approaches for XPCi that, through a simple modification of the EI setup, provide an effective method to retrieve absorption, refraction, and scattering signals of a sample from the beam intensity profile acquired through a high resolution detector. The virtual edge approach can be easily combined with existing
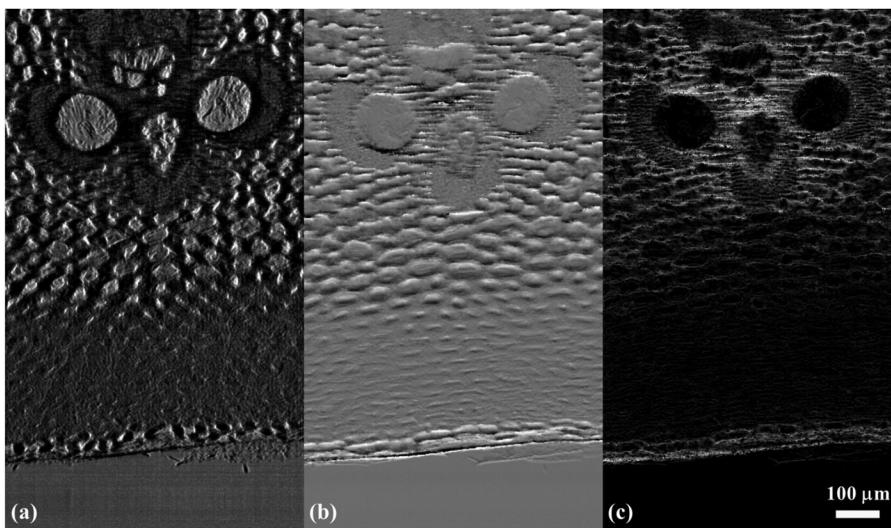

FIG. 4. Absorption (a), refraction (b), and scattering (c) images of a bamboo wood slice obtained with the beam tracking method.

phase retrieval techniques developed for EI, providing similar image quality while allowing a reduction of exposure time and delivered dose. The beam tracking approach, at the cost of a more elaborate and computationally demanding data analysis, improves the results of the virtual edge approach by additionally providing the scattering signal.

[1]U. Bonse and M. Hart, "An x-ray interferometer," Appl. Phys. Lett. **6**, 155–156 (1965).

[2]A. Snigirev, I. Snigireva, V. Kohn, S. Kuznetsov, and I. Schelokov, "On the possibilities of x-ray phase contrast microimaging by coherent high-energy synchrotron radiation," Rev. Sci. Instrum. **66**, 5486–5492 (1995).

[3]V. N. Ingal and E. A. Beliaevskaya, "X-ray plane-wave topography observation of the phase contrast from a non-crystalline object," J. Phys. D: Appl. Phys. **28**, 2314–2317 (1995).

[4]A. Olivo, F. Arfelli, G. Cantatore, R. Longo, R. H. Menk, S. Pani, M. Prest, P. Poropat, L. Rigon, G. Tromba, E. Vallazza, and E. Castelli, "An innovative digital imaging set-up allowing a low-dose approach to phase contrast applications in the medical field," Med. Phys. **28**, 1610–1619 (2001).

[5]C. David, B. Nohammer, H. H. Solak, and E. Ziegler, "Differential x-ray phase contrast imaging using a shearing interferometer," Appl. Phys. Lett. **81**, 3287–3289 (2002).

[6]F. Pfeiffer, T. Weitkamp, O. Bunk, and C. David, "Phase retrieval and differential phase-contrast imaging with low-brilliance x-ray sources," Nat. Phys. **2**, 258–261 (2006).

[7]A. Olivo and R. Speller, "A coded-aperture approach allowing x-ray phase contrast imaging with conventional sources," Appl. Phys. Lett. **91**, 074106 (2007).

[8]L. Rigon, F. Arfelli, and R. H. Menk, "Generalized diffraction enhanced imaging to retrieve absorption, refraction and scattering effects," J. Phys. D: Appl. Phys. **40**, 3077–3089 (2007).

[9]M. Endrizzi, P. C. Diemoz, T. P. Millard, J. L. Jones, R. D. Speller, I. K. Robinson, and A. Olivo, "Hard X-ray dark-field imaging with incoherent sample illumination," Appl. Phys. Lett. **104**, 024106 (2014).

[10]P. C. Diemoz, M. Endrizzi, C. E. Zapata, Z. D. Pesic, C. Rau, A. Bravin, I. K. Robinson, and A. Olivo, "X-ray phase-contrast imaging with nanoradian angular resolution," Phys. Rev. Lett. **110**, 138105 (2013).

[11]P. R. T. Munro, C. K. Hagen, M. B. Szafraniec, and A. Olivo, "A simplified approach to quantitative coded aperture X-ray phase imaging," Opt. Express **21**, 11187–11201 (2013).

[12]S. W. Wilkins, "Improved x-ray optics, especially for phase contrast imaging," International patent WO 1995005725 A1 (February 23 1995).

[13]K. S. Morgan, D. M. Paganin, and K. K. W. Siu, "X-ray phase imaging with a paper analyzer," Appl. Phys. Lett. **100**, 124102 (2012).

[14]K. S. Morgan, P. Modregger, S. C. Irvine, S. Rutishauser, V. A. Guzenko, M. Stampanoni, and C. David, "A sensitive x-ray phase contrast technique for rapid imaging using a single phase grid analyzer," Opt. Lett. **38**, 4605–4608 (2013).